Journal of Power Sources, 40 (1992) 125–136

Premature capacity-loss mechanisms in lead/acid batteries

A. F. Hollenkamp*, K. K. Constanti, A. M. Huey, M. J. Koop and L. Aputeanu**
CSIRO Division of Mineral Products, Port Melbourne, Vic. 3207 (Australia)

Abstract

The phenomenon known as 'premature capacity loss' (PCL) causes the early demise of lead/acid batteries based on a variety of grid alloys. It is also known to be a problem specific to the positive plate and is usually invoked by duties that involve repetitive deep-discharge cycling. In order to determine the cause(s) of the problem, an extensive study of the behaviour of cells based on a range of positive grid alloys is being conducted. Examples of PCL have been generated by subjecting three-plate cells to 100% depth-of-discharge, at $I = C_8/8$, with 110% overcharge. Cells based on antimony-free grids exhibit capacity loss at a rate of up to 5% of the initial capacity per cycle, with both constant-current and constant-voltage charging. With the latter charging method, most of the cells also develop extremely poor charge acceptance within 10 to 15 cycles. The performance of cells with high-antimony positive grids is significantly better, although substantial capacity loss is still observed. The latter cannot be explained by any of the classic failure modes for lead/acid batteries. Poor charge acceptance is not displayed by these cells. Plates show signs of physical degradation, but these represent a minor contribution to capacity loss. Phase composition of positive material does not vary with grid alloy and is typical of healthy plates. Investigations of corrosion-layer morphology have shown that Pb–Ca grids give rise to weak corrosion products that are prone to fracture and separation, while the corrosion layers on Pb–Sb plates are apparently more coherent and more strongly bonded to the underlying grid.

Introduction

Following the widespread introduction of antimony-free grid alloys for maintenance-free lead/acid batteries, premature capacity loss (PCL) has developed as a major research topic [1]. Despite the sustained research effort, a full understanding of the mechanism(s) that constitute PCL has not yet been achieved. To this end, the International Lead Zinc Research Organization (ILZRO) and CSIRO are conducting a joint research project on the cause(s) of, and remedies for, PCL. The first goal has been to generate, reproducibly, examples of PCL under controlled experimental conditions. The affected cells provide samples for chemical, electrochemical and structural investigations of the underlying mechanisms. From here, the project will move to a consideration of methods for overcoming capacity loss. This paper presents a summary

*Author to whom correspondence should be addressed.
**On leave from the Chemical and Biochemical Energetics Institute of Bucharest, Bucharest, Romania.

0378-7753/92/$5.00

of the results obtained to date, along with an indication of the direction for future work.

Experimental programme

The experimental basis for this study is the production of lead/acid cells in which as many as possible of the normal manufacturing variables are controlled. Since PCL is due to changes in the properties of the positive plate the principal variable under investigation is the composition of the positive grid alloy. Table 1 provides a summary of the alloys that are under examination.

The grid is a light motive-power type with the following dimensions: 121 mm (height) × 143 mm (width) × 3.2 mm (thickness). The average weight of each grid is ~116 g. The cast grids are supplied by East Penn Manufacturing Co. Inc., (Lyon Station, PA). The chosen range of alloy composition allows a comparative evaluation of the effect(s) of calcium, tin and antimony on plate performance. Details of paste preparation and curing for the positive plates are summarized in Fig. 1. The paste is based on an Australian Barton-pot leady oxide and follows a formula that consistently gives a wet-paste density close to 4.1 g cm^{-3}. Curing is carried out at 50 °C in 100% relative humidity and yields a two-component cured state consisting of α-PbO and tribasic lead sulfate (3BS). Dry, cured positive plates are enveloped by polyethylene separators (with a glass mat lining) and placed in polypropylene cases with matching negative plates. The latter are provided in the cured state by East Penn Manufacturing Co. and feature a low-tin Pb–Ca alloy. Cells consist of three plates (viz., one positive and two negative plates) which are immersed in 1.27 sp. gr. sulfuric acid. Cell formation follows the current profile shown in Fig. 2, at a constant temperature of 40 °C. Formed positive material is found to have the following phase composition: 9wt.%α-PbO_2–86wt.%β-PbO_2–5wt.%$PbSO_4$. Cells are configured with an excess of 1.27 sp. gr. electrolyte (~6 ml per g of positive material).

Several different duties have been used to demonstrate PCL [1]. With the exception of the submarine cycle used by the US Naval Research Laboratories [2–5], most studies of PCL have been based on deep-discharge regimes with discharge times of at least 5 h. The work reported here utilizes a discharge current of 2.5 A per positive plate. This yields a discharge time of around 8 h for a healthy cell (i.e., $I = C_8/8$). The end-of-discharge voltage is 1.75 V and this corresponds to 100% depth-of-discharge (DOD).

TABLE 1

Composition of grid alloys

Alloy	Constituent (wt.%)		
	Ca	Sn	Sb
pure Pb			
Pb–Ca	0.09		
Pb–Ca–Sn-1	0.09	0.32	
Pb–Ca–Sn-2	0.09	0.70	
Pb–Sb-1		0.35	1.64
Pb–Sb-2		0.061	1.66
Pb–Sb-3		0.27	5.73

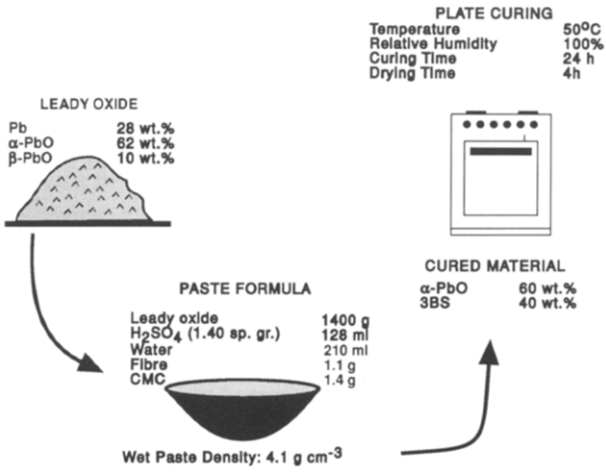

Fig. 1. Schematic representation of paste preparation and plate curing.

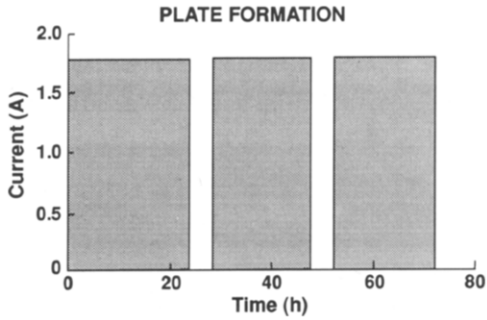

Fig. 2. Current/time profile for plate formation.

Initially, the cycling regime was configured with a constant-current/constant-voltage (CC–CV) charging procedure in which the current was held at 2.5 A until the cell voltage reached 2.55 V, after which the voltage was maintained at 2.55 V. Charging was terminated once the ratio of the amount of charge put in to the amount removed (in the previous discharge) reached 1.1. As will be seen later, most of the antimony-free cells exhibited very poor charge acceptance under the CC–CV procedure. In order to investigate the effect(s) that charge acceptance was exerting on cell performance, a second method of charging has been devised. The latter is a two-step constant-current (CC) procedure, in which there is no upper voltage limit. Charging is fixed at 1.0 A until the voltage reaches 2.55 V, at which point the current drops to 0.5 A. Again, an amount of charge equal to 110% of the previous discharge is returned.

In general, it has been decided to terminate charge/discharge service when the capacity has fallen to approximately 50% of the initial value. At this stage, all plates are washed with distilled water, until substantially free of sulfuric acid, then dried at 105 °C. Samples may then be taken from the positive plates for the required analyses. Those for examination by scanning electron microscopy (SEM) are taken in a two-step process. The procedure is illustrated in Fig. 3. First, small portions of the plate are removed by careful excision (Fig. 3(a)). The excised portion consists of a grid wire and a 'pellet' of positive material. The pellet is broken away from the adjacent

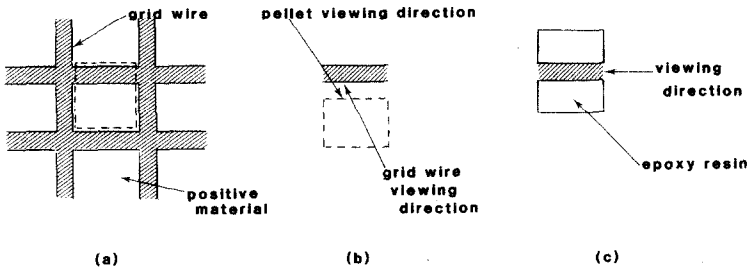

Fig. 3. Preparation of samples for scanning electron microscopy: (a) portion removed from plate; (b) pellet and grid wire separated for examination, and (c) grid wire mounted for cross section.

grid wire and the exposed surfaces (grid and pellet) are examined (Fig. 3(b)). This technique yields microscopically rough samples and focuses attention on the region of the sample close to the grid that is mechanically the weakest. The location in which the sample has broken, and the disruption apparent in subsequent viewing, both provide a measure of: (i) the strength and cohesion of the material, and (ii) the strength of the bond between the material removed and the substrate. Typically, the morphology of the exposed surface is heterogeneous due to: (i) adherence of some porous (bulk) material to the corrosion layer, and (ii) cleavage of the corrosion layer away from the grid surface, thereby exposing bare grid metal. The second stage of sample preparation involves mounting the remainder of the positive plate in epoxy resin and then polishing cross sections of the mounted plate with successively finer abrasives. The grid wire isolated in the first step can also be mounted in epoxy resin and then sectioned so as to reveal a cross-sectional view of the adhering material (Fig. 3(c)).

Quantitative phase analysis of the crystalline fraction of positive plate material was conducted by means of X-ray diffraction (XRD) methods developed by CSIRO. Diffraction patterns were recorded on a Philips (Eindhoven, Netherlands) Model PW17 diffractometer equipped with a Cu Kα X-ray source. Electron micrographs were obtained with a JEOL (Tokyo, Japan) Model JSM-25S III microscope operated at an accelerating voltage of 25 kV and at a working distance of $\sim$10 mm. Cell internal resistance was measured by two methods. The first involves the determination of the drop in cell voltage that occurs when a galvanostatic discharge pulse of very brief duration (typically 100 μs) is applied to a cell. The magnitude of the resulting voltage transient is proportional to the cell resistance. The second method employed the Yokogawa-Hewlett-Packard (Tokyo, Japan) Model HP 4338A milliohmmeter. This instrument measures resistance by applying a small a.c. perturbation and measuring the resulting variation in voltage. Both methods yielded essentially the same results.

Results

To date, 22 cells have completed service under the CC–CV charging procedure. Cells based on each of the alloys in Table 1 exhibited loss of capacity over periods of up to 60 charge/discharge cycles. The most severe decline in capacity occurred for the cells made with pure lead grids; up to 5% of initial capacity was lost per cycle. Those based on the Pb–5.7wt.%Sb–0.3wt.%Sn alloy suffered the lowest rate of capacity loss; $<1\%$ of initial capacity per cycle. The behaviour of cells with the tin-free Pb–Ca positive grid alloy was, on average, intermediate between that recorded for the antimonial

and pure lead cells. This is not, however, a complete description of the situation, because the influence of another important parameter of battery performance was recorded during the charge/discharge programme, viz., charge acceptance.

The comparison of antimonial and nonantimonial cells revealed substantial differences in charge acceptance. Specifically, most of the latter cells exhibited very low charging current once the constant-voltage regime was entered. This behaviour was never present in fresh cells, but developed during the first ten cycles. In many cases, the current fell to close to the detection limit of the charge-control equipment and, thereby, extended greatly the length of time required for complete charging of the cell. The time spent in constant-voltage charging is, therefore, a good indicator of charge acceptance and several plots of this parameter have been constructed.

Figure 4 summarizes the charge-acceptance characteristics of the cells. The data for cell PR36-1 (pure lead positive grid) are used as an example of the behaviour of antimony-free types. The resulting profile of constant-voltage charging (CVC) time, against cycle number, exhibits a large and steady increase from the start of operation. Eventually, the CVC time reaches a maximum value that is maintained in most of the subsequent cycles. This plateau behaviour may not be due to any particular cell characteristic because the control software requires a maximum CVC time to be set; for cell PR36-1, this was 33 h (indicated by the dashed line in Fig. 4). With a higher limit, CV charging would have extended for longer periods. While most of the antimony-free cells displayed a substantial increase in CVC time early in cycle life, it should be noted that some of these did not sustain long CVC times throughout their entire cycle life. Rather, the CVC time, after reaching a high value, underwent a sharp drop to a value close to that registered for the first cycle. Further, a very small number of cells did not develop long CVC times at all. Thus, there is clearly some variability in the data for antimony-free cells and more information on the nature and extent of poor charge acceptance is needed.

For cells with Pb–5.7wt.%Sb–0.3wt.%Sn positive grids, the results exhibited little variance and this allowed the data to be plotted as an average for all the cells examined. The resulting curve is given in Fig. 4. No individual CVC times exceeded 12 h, nor did any reach the programmed maximum value. CVC time increases during the first few cycles, but the effect is small in comparison with that found in nonantimonial cells.

Having identified charge acceptance as an important issue, investigations of the internal resistance (IR) of cells was incorporated into the experimental programme. New cells begin service with an IR = 5 to 7 mΩ and display a slight increase, reaching

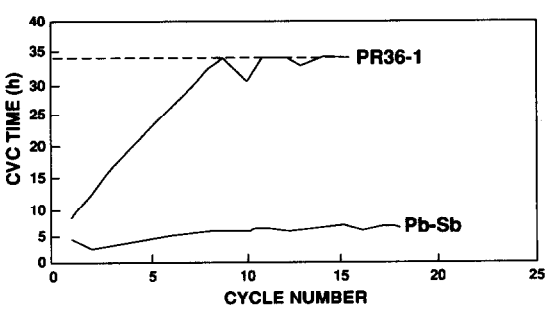

Fig. 4. Plots of constant-voltage charging (CVC) time vs. cycle number for a typical nonantimonial cell (PR36-1) and the averaged data for Pb–5.7wt.%Sb–0.3wt.%Sn cells.

IR = 7 to 9 mΩ, within ~30 cycles. At present, these data are recorded at open circuit, after full charging. To date, no differences have been observed in IR between cells of the various alloys. Circuitry has recently been developed in our laboratories that will allow continual measurements of IR during charge/discharge cycling.

Following the observation and characterization of poor charge acceptance in the antimony-free cells, it was decided to investigate the behaviour of cells under conditions where this phenomenon would not be able to influence greatly the time required for charging. A major concern was that the charging of these cells for such long times could possibly enhance the retention of capacity to some degree. Certainly, no industrial usage of cycling lead/acid batteries would tolerate such long charging times, so a procedure to remove this feature was needed. As already noted, the principal cause of long charging periods is the constant-voltage component. Removal of the upper voltage limit (2.55 V), and imposition of a two-step current regime, led to similar charging times for antimonial and nonantimonial cells. At that juncture in the work programme, the decision was also taken to focus attention on two of the grid alloys: Pb–5.7wt.%Sb–0.3wt.%Sn and Pb–Ca–0wt.%Sn, hereafter referred to as Pb–Sb and Pb–Ca, respectively. The performance of cells with positive plates based on these alloys is summarized in Fig. 5. Data are plotted as an average for each alloy. The average for Pb–Ca and Pb–Sb represents ten and eight cells, respectively.

After the first few cycles, the discharge capacity for the Pb–Sb cells falls steadily to ~50% of the initial value, over a period of ~50 cycles. By comparison, the Pb–Ca cells suffer the same degree of capacity loss in approximately half the number of cycles. Hence, the rate of capacity decline for Pb–Ca is approximately twice that for Pb–Sb under constant-current charging. These results are similar to those obtained under CC–CV charging in that the two alloy systems differ in the rate of capacity loss observed.

The condition of the positive plates at the end of cycling (with either charging regime) was the subject of detailed investigation. Visual inspection revealed some buckling (warping) but, for most alloys, this was neither severe nor always present. Plates based on pure lead grids exhibited the most consistent and noticeable buckling at failure. In more recent work with the two-step CC charging procedure, plates with Pb–Ca grids displayed a greater degree of buckling than those with Pb–Sb grids. The extent of the distortion was, however, variable and, importantly, there was no correlation with the rate of capacity loss. The loss of positive material ('shedding') was also assessed for failed plates. On average, more material was shed from Pb–Sb than from

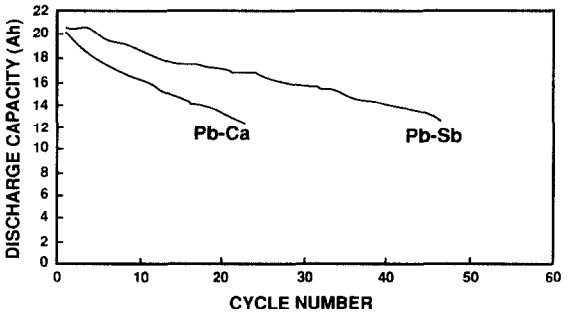

Fig. 5. Discharge capacity vs. cycle number for Pb–Sb and Pb–Ca cells charged by the two-step constant-current procedure.

Pb–Ca cells, viz., 20 versus 10% of the total porous mass. As anticipated, it has not been possible to remove entirely the common physical modes of degradation such as plate distortion and material loss. On the contrary, these processes are always present and their influence on plate performance increases with cycle life. This topic is discussed below.

In the next stage of investigation, samples of positive plate material were removed for phase analysis. It was found that the phase composition was remarkably consistent throughout the entire range of cycled cells and showed no variation with different grid alloying elements. The data, expressed as a range of values for each phase, are as follows: 1-3wt.%α-PbO_2–96-99wt.%β-PbO_2–0-2wt.%$PbSO_4$. Thus, the abundance of the alpha polymorph decreased during cycling (see composition of formed plates, above), as expected. In addition, the material contained remarkably low levels of lead sulfate. Chemical analysis of selected samples was conducted in order to determine the total abundance of this compound in the material. (Note, XRD methods are only able to quantify crystalline material above a minimum crystallite size.) The results showed that samples judged by XRD to be free of lead sulfate actually contain 2 wt.% of the compound. Similarly, material with 1 wt.% lead sulfate by XRD was shown to contain 3 wt.% by chemical analysis. Thus, it is clear that cycled positive material contained a small amount of lead sulfate that is either amorphous or comprised of very small crystallites. Previous examples of this phenomenon have been reported in ref. 6.

Examination of cycled positive plates also included extensive investigations of structural and morphological features of plate material, by means of SEM. To date, several examples of plates based on the Pb–Sb and Pb–Ca grid alloys have been studied. Significantly, consistent and distinct trends in the microscopic characteristics for the two systems are emerging, and these will be outlined in the following discussion by reference to samples from two particular cells.

Samples from Pb–Ca positive material have been shown to be susceptible to fracture of material in the corrosion layer. This often leads to exposure of the grid. Figure 6 shows a view of the grid-corrosion layer for one of the samples removed from the positive plate of a cycled Pb–Ca cell. The image centres on a region in which grid metal has been exposed. Bare grid fills the upper third of the image, a band across the middle of the image reveals views of the fractured corrosion layer and the lower portion consists of porous (bulk) positive material. This image is one of many similar images obtained from a variety of samples and shows remarkable detail of the corrosion products and their bonding to adjacent materials. In summary, the important aspects of the image are: (i) the corrosion layer is bilayered and interlayer fracture is prominent; (ii) detachment of the inner corrosion layer from the grid is apparent, and (iii) bonding of porous positive material to the outer corrosion layer is apparently strong.

Further information is obtained by also examining the surface of the pellet that was detached from the grid wire. A representative image is shown in Fig. 7. The material that occupies the upper left side of the micrograph appears to be a section of outer corrosion layer that has adhered to the pellet during sample preparation. It can be seen that the surface of this material (exposed by detachment from the grid/corrosion layer) is quite smooth and there is little sign of particulate structure.

Several positive plates based on the high-antimony alloy have been examined by the same method. Figure 8 provides a typical view of the grid-corrosion layer region. Importantly, inspection of the broken surface of the grid-based samples seldom revealed any sign of exposed grid metal. The image in Fig. 8 is characterized by large (tens

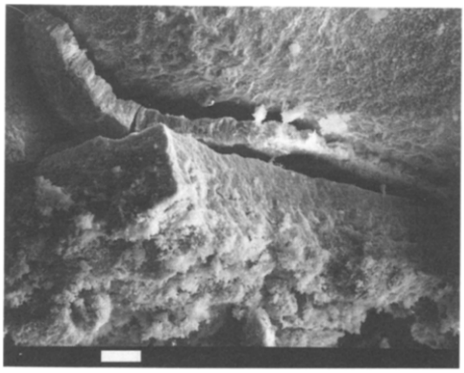

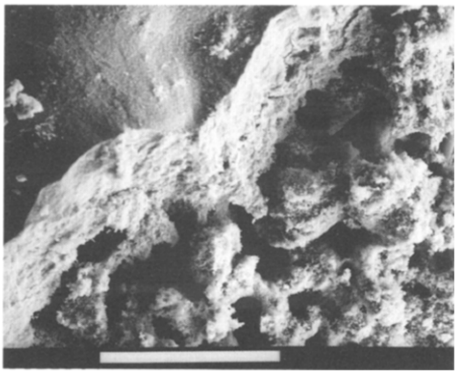

Fig. 6. Secondary-electron micrograph of the surface of the grid-corrosion layer sample from a cycled Pb–Ca positive plate; bar length: 10 μm.

Fig. 7. Micrographs of the cleaved surface of the pellet broken away from the grid-based sample in Fig. 6; bar length: 100 μm.

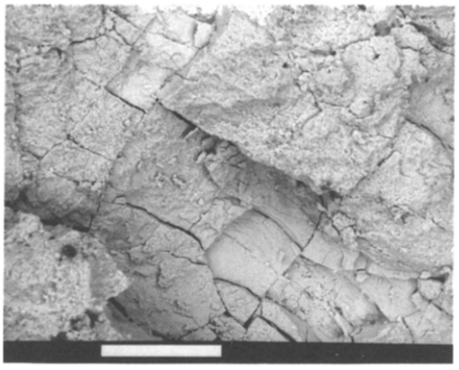

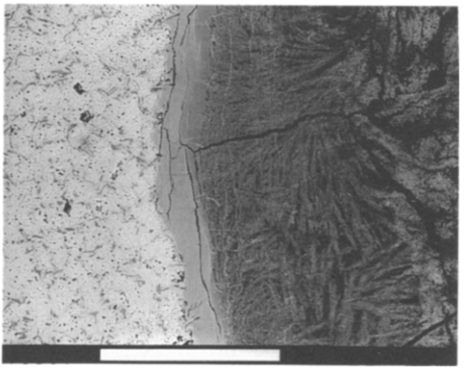

Fig. 8. Backscattered-electron micrograph of the grid-corrosion layer sample from a cycled Pb–Sb positive plate; bar length: 100 μm.

Fig. 9. Backscattered-electron micrograph of a cross section from the same positive plate as in Fig. 8; bar length: 100 μm.

of microns) block-like formations that, upon examination at higher magnification, are shown to have a fine structure composed of sub-micron-sized particles. These block agglomerates exhibit much denser packing of constituent particles than that seen in the pellet, far from the grid. Thus, images such as Fig. 8 are probably showing features of the material in the corrosion layer, close to the grid.

For comparison, Fig. 9 shows a view of a polished cross section from the same plate. From left to right, the image passes from grid, through corrosion layer to porous active material. It is apparent that the porous material is closer packed and more ordered adjacent to the dense corrosion layer than that further away from the grid. Various stresses within the plate have caused fracture of the material in and around the corrosion layer. The resultant cracks have: (i) separated porous material from the dense corrosion products; (ii) penetrated the corrosion layer, and (iii) not caused separation of corrosion products from the grid. Thus, the bonding between the grid

and the corrosion layer is apparently much stronger than for Pb–Ca samples. The result of this is that preparation of 'rough' samples only exposes material in the corrosion layer, as indicated by Fig. 8.

Discussion

Premature capacity loss has been demonstrated in a reproducible manner under the controlled conditions of the experimental regime. Under two different charging procedures, CC–CV and two-step CC, PCL is expressed as an almost linear decrease in discharge capacity that commences at the beginning of service. It will be argued that PCL is being demonstrated in both antimony-free positive plates and those based on a grid alloy with a relatively high content of antimony (5.7 wt.%). Such a view is contentious, but before pursuing the discussion further, the results of examinations of failed plates will be analysed so that a judgement can be made on the principal cause of failure. The magnitude of modes of plate degradation, other than PCL, must be assessed and placed in proper perspective.

First, data collected on the phase composition of positive plate material indicate little or no variation between samples from cells with different grid alloys. The samples are also largely free of lead sulfate. This rules out mechanisms of capacity loss founded on bulk sulfation of the positive mass. The other likely degradative processes that afflict positive plates are essentially mechanical in nature. The most common of these are: (i) loss of material from the plate (shedding); (ii) weakening and eventual fracture of grids due to corrosion, and (iii) distortion of grids due to growth/buckling. Given the observed condition of plates in this study, the following conclusions can be drawn: (i) shedding of positive material amounts to $\sim 20\%$ of the porous mass for Pb–Sb plates and to $\sim 10\%$ for Pb–Ca plates; (ii) grid weakening, leading to fracture of grid wires, it a rare occurrence. It is probably associated with casting defects in the grids, and (iii) distortion of the plates due to grid buckling is present in many failed plates; Pb–Ca plates exhibit a greater degree of buckling than Pb–Sb equivalents.

Several associated points must also be mentioned. First, there was no relationship between the degree of plate distortion and either the amount of shedding or the rate of capacity loss. This point is particularly relevant to Pb–Ca cells for which, at first sight, it might have been suggested that the greater extent of distortion was causing capacity loss. Such a conclusion is not justified by the data. Rather, it is believed that distortion is not contributing significantly to the decrease in performance of either Pb–Ca or Pb–Sb cells. Second, the amount of material that shed from the positive plate exhibited a reasonable correlation with the number of cycles completed. This is exemplified by the observation that shedding was approximately twice as severe for Pb–Sb plates as for Pb–Ca analogues and the cycle lives of the former were, on average, twice those of the latter (Fig. 5). This is a relationship that is often found for lead/acid batteries operated under deep-cycling conditions. For the Pb–Sb cells in this study, it is clear that shedding makes a significant contribution to plate degradation. By contrast, shedding makes a minor contribution to the capacity lost by these cells because it explains less than half of the drop in discharge capacity. Other, hidden, processes provide the major contribution. Thus, it is suggested that even high-antimony cells are susceptible to modes of capacity loss that are still to be explained. Describing the latter as PCL, however, appears to clash with many common perceptions of the problem.

It is widely believed that cells based on high (>5 wt.% Sb)-antimony positive grid alloys will always provide good performance under repetitive deep-cycle service.

The common interpretation of the term 'good performance' is that cycle life will begin with at least several cycles in which the discharge capacity remains at or above the nominal value. This will be followed by a very gradual decrease in capacity due to the well-known processes of plate degradation, such as grid corrosion and material shedding. Behaviour like this is often observed, but invariably under conditions in which the utilization of the positive plate material is relatively low. The reason for this situation is that the discharge capacity of lead/acid cells for cycling duty is usually limited by the amount of negative material and/or the quantity of sulfuric acid present. (Note, positive material utilization (PMU) = actual discharge capacity/theoretical maximum capacity.)

In the present study, cells are configured with a substantial excess of both sulfuric acid and negative material. This ensures that PMU is relatively high; examination of capacity data yields values in the range of 55 to 60%. In their extensive research into capacity loss, workers at Varta Batterie AG (Kelheim, Germany) also provided [7, 8] a detailed account of the performance of lead/acid cells under conditions of high utilization. Studies with the Eloflux cell, in which forced flow of an excess of electrolyte generated high-material utilization, showed that positive plates based on a typical high-antimony alloy can lose over 50% of capacity within 30 deep-discharge cycles. Plates with low-antimony and Pb–Ca alloys lost capacity at even greater rates. These findings are in agreement with those reported here.

Clearly, repetitive deep-discharge cycling of any type of lead/acid cell at high levels of PMU will accelerate capacity loss. The Varta group have offered an explanation of this behaviour in terms of their theory of relaxable insufficient mass utilization (RIMU) of which PCL is an important manifestation [8]. No distinction is made between the capacity loss observed in high-antimony, low-antimony or antimony-free systems because each is due to the same process, namely, a diminution of positive material conductivity that is labelled RIMU. Another school of thought believes that PCL is due to the development of electrical barriers close to the grid [9–14]. Most studies propose that these barriers comprise nonconducting compounds such as $PbSO_4$ and α-PbO. Further, a popular theory of barrier formation states that a continuous layer of $PbSO_4$ is required to establish the conditions of high pH needed for the production of α-PbO [15, 16]. Electrical barriers may also be generated simply by cracking and separation of material in the corrosion layer [12–14]. Our results suggest that there is probably considerable overlap between these two aspects of the barrier theory. Indeed, the observation of discrete layers near the grid is consistent with earlier reports of barrier compounds, and the same material is also clearly prone to separation under stress. Both types of barrier will cause capacity loss by preventing large portions of the positive material from participating in further reaction.

By comparison with the work at Varta, reports that argue the 'barrier layer' theory tends to either claim, or imply, that positive plates based on high-antimony grids are not subject to the formation of barrier layers. We believe, however, that there is little real support for this argument. With the exception of the Varta work, few previous studies of capacity loss under deep-cycling service have considered the comparative behaviour of high-antimony cells. Of these, none has exposed cells to high PMU, with the result that high-antimony cells have not experienced the conditions that cause severe capacity loss. The main point here is that because antimonial cells are more resistant to the processes of capacity loss, the limitation to their performance (apart from the well-characterized modes of failure) can only be exposed at high PMU. The reason for this limitation is unclear, however, and barrier layer formation cannot be ruled out.

At the same time, the presentation of micrographs from our study of corrosion-layer morphology is not intended to give the impression that we favour the barrier theory.

Rather, this region of interest has proven, initially, to be the most amenable to detailed investigation. Early results have identified differences in the physical properties of the corrosion products derived from Pb–Ca and Pb–Sb plates. Yet, the interpretation of these differences is complicated by the knowledge that the antimony-based samples have also been affected by capacity loss. In order to arrive at a complete explanation of PCL, phenomena that cause capacity loss in all types of positive plate, including those based on alloys with high-antimony contents, must be considered. For this reason, strategies for investigating the important area of active material conductivity are already under development.

Conclusions

The results obtained to date have highlighted several important aspects of PCL:
(i) PCL occurs under two distinctly different charging regimes: constant/current–constant-voltage (CC–CV) and a two-step constant-current method. Until now, the influence of charging procedure on the incidence of PCL had not been investigated in detail.
(ii) the CC–CV procedure has demonstrated that poor charge acceptance is usually noted for antimony-free cells. This suggests that the choice of charging method for these cells can affect greatly the resulting performance.
(iii) PCL affects Pb–Sb (high-antimony) cells but the rate of capacity loss is half that of Pb–Ca cells. Whether the same mechanism(s) of capacity loss are operative is unclear.
(iv) The phase composition of positive material from failed cells is constant across the range of grid alloys. All samples contain low levels of lead sulfate which rules out large-scale sulfation of the positive material as the mode of failure.
(v) Corrosion products in Pb–Ca samples are less coherent and more prone to fracture than those from Pb–Sb equivalents.

Future work

The above remarks indicate that further work in several key areas must be conducted in order to reach a complete understanding of PCL. In particular, emphasis in the experimental programme is currently being devoted to the search for techniques that can offer new information on lead/acid cell operation. At present, encouraging results are being obtained with an electrochemical technique for characterizing the electrical properties of plate materials, *in situ*. The technique, known as 'cyclic resistometry' and developed in the CSIRO laboratories [17], makes use of the voltage transient that arises when a large-amplitude current pulse is passed through the electrochemical cell. The response is sensitive to the electrical properties (resistance, capacitance, etc.) exhibited by the working electrode. Other studies are aimed at incorporating a range of species-sensing devices (e.g., H^+, SO_4^{2-}) into the positive plate. An important focus for this work is that the production of α-PbO barrier layers would require the establishment of high pH conditions near the grid.

Acknowledgements

The authors wish to thank Dr D. A. J. Rand for useful discussion of the results and Mr J. A. Hamilton for construction and development of the device for IR measurement.

References

1 A. F. Hollenkamp, *J. Power Sources, 36* (1991) 567.
2 J. Burbank, *J. Electrochem. Soc., 111* (1964) 765.
3 J. Burbank, *J. Electrochem. Soc., 111* (1964) 1112.
4 J. Burbank and E. J. Ritchie, *J. Electrochem. Soc., 116* (1969) 125.
5 J. Burbank and E. J. Ritchie, *J. Electrochem. Soc., 117* (1970) 299.
6 K. Harris, R. J. Hill and D. A. J. Rand, *J. Electrochem. Soc., 131* (1984) 474.
7 W. Borger, U. Hullmeine, H. Laig-Hörstebrock and E. Meissner, in T. Keily and B. W. Baxter (eds.), *Power Sources 12*, International Power Sources Symposium Committee, Leatherhead, Surrey, UK, 1989.
8 A. Winsel, E. Voss and U. Hullmeine, *J. Power Sources, 30* (1990) 209.
9 S. Tudor, A. Weisstuch and S. H. Davang, *Electrochem. Technol., 3* (1965) 91.
10 S. Tudor, A. Weisstuch and S. H. Davang, *Electrochem. Technol., 4* (1966) 406.
11 S. Tudor, A. Weisstuch and S. H. Davang, *Electrochem. Technol., 5* (1967) 21.
12 H. Nakashima and S. Hattori, *Proc. Pb80, 7th Int. Lead Conf., Madrid, May 12–15, 1980,* p. 88.
13 T. G. Chang, in K. R. Bullock and D. Pavlov (eds.), *Proc. Symp. Advances in Lead-Acid Batteries, Vol. 84-14,* The Electrochemical Society Inc., Pennington, NJ, 1984, pp. 86–97.
14 K. Gibson, K. Peters and F. Wilson, in J. Thompson (ed.), *Power Sources 8,* Academic Press, London, 1981, p. 565.
15 D. Pavlov and N. Iordanov, *J. Electrochem. Soc., 117* (1970) 1103.
16 P. Ruetschi, *J. Electrochem. Soc., 120* (1973) 331.
17 R. L. Deutscher, S. Fletcher and J. A. Hamilton, *Electrochim. Acta, 31* (1986) 585.